Journal of The Electrochemical Society, **159** (4) K78-K82 (2012)
0013-4651/2012/159(4)/K78/5/$28.00 © The Electrochemical Society

Core-Shell Ni-NiO Nano Arrays for UV Photodetection without an External Bias

Chien-Min Liu, Chih Chen,[z] and Yuan-Chieh Tseng

Department of Materials Science and Engineering, National Chiao-Tung University, Hsinchu 30010, Taiwan

This work demonstrates a simple method for fabricating a nano-structured device that performs notable photodetecting capabilities. With a template of anodic aluminum oxide, highly ordered Ni-NiO nano core-shell arrays were fabricated by annealing the electroless-deposited Ni arrays at 300°C for 30 minutes. High-resolution transmission electron microscopy (HRTEM) demonstrated that a NiO layer with a thickness of ∼5 nm was developed on the surface of the Ni arrays. The effects of annealing time and temperature on NiO were probed by HRTEM. Results show that temperature has a greater effect on the development of NiO. The Ni/NiO interface forms naturally a Schottky nanojunction, which covers most of the array surface when patterned with an indium-tin oxide (ITO) electrode. The ITO/Ni-NiO/Si device was found to yield photocurrent when exposed to ultraviolet (UV) light without an external voltage bias. The device takes great advantage of the large junction area and one-dimensional configuration of the core-shell array, displaying rapid photoresponse to UV light and subsequent steady photocurrent. These features make the proposed device a viable alternative to the UV photodetector.
 [DOI: 10.1149/2.067204jes]

Manuscript submitted October 7, 2011; revised manuscript received January 13, 2012. Published January 31, 2012.

Attention to photoconductive materials has been on the rise in recent years, with growing awareness that the conversion from photons to electrons through a material's light-absorbing process has wide application in military, aerospace, environmental, and biological settings.[1–5] Apart from the search for photoconductive materials with low cost, high efficiency, and ease of fabrication,[6–12] shaping these materials with a low-dimensional framework, namely nanostructure, has been found to enhance efficiently the sensitivity of materials to ultraviolet (UV) light.[13,14] The increase in sensitivity is attributed to the large surface-to-volume ratio of the nanostructure.[13,15] This discovery has brought attention to the effect of structural configurations, sizes, and distributions of materials on their photoconductive properties.[16–19]

To date, most of the advancements in the material front have come about through chemical synthesis.[20–24] Despite the promising performance exhibited by chemically synthesized materials, their fabrication involves catalyzes that are too complex and costly for industrial use. Moreover, materials manufactured through chemical means usually lack high natural ordering,[20,22–24] making them hard to integrate with traditional semiconductors. In addition, it is reported that photodetectors with Schottky contacts can significantly enhance the sensitivity.[25,26]

In order to achieve the requirements of high sensitivity, we hereby propose a Ni-NiO core-shell nanostructured device, which is simple to fabricate and has notable capabilities, as an alternative to the UV photodetector. We demonstrate that with post-annealing, the Ni nano-arrays were naturally coated by a uniform NiO shell, forming a core-shell structure featuring a Schottky junction between the semiconductor (NiO) and the metal (Ni). The nano-arrays were grown directly on the Si substrate by electroless-deposition,[27] implying that their manufacture could be incorporated with that of traditional semiconductors. High-resolution transmission electron microscopy (HRTEM) revealed the relationships between the microstructure of the Ni/NiO interface and the device's electrical and photoconductive properties. Surprisingly, the device yielded detectable photocurrent without an external voltage bias. The device responded to UV illumination in less than one second, and the generated photocurrent was steady. These advantages are attributed to the device's unique nanostructure and make it a viable alternative to the UV photodetector.

Experimental

To begin, an anodic aluminum oxide (AAO) template with pores of about ∼70 nm was prepared on a *p*-type Si substrate by following the method previously reported.[28] Prior to the electroless deposition process, the AAO-Si sample was sensitized and activated by a $SnCl_2$/HCl solution (40 g/L $SnCl_2$ + 3 mL/L HCl) and a $PdCl_2$/HCl solution (0.15 g/L $PdCl_2$ + 3 mL/L HCl). The electroless plating solution was composed of $NiSO_4$ as the main Ni source, NaH_2PO_2 as the reducing agent, $Na_2C_4H_4O_4$ as the stabilizing agent, and $Pb(NO_3)_2$ as the buffer agent. The operating conditions of the electroless deposition had been introduced in previous research.[29,30]

After the removal of the AAO template, the Ni/Si samples were sent to post-annealing at 300°C for 30 minutes in atmospheric conditions to develop Ni-NiO core-shell arrays. Transmission electron microscopy (TEM, JEM-2100F) and high-resolution (HR) imaging probed the microstructure of the arrays and Ni/NiO interface. Energy-dispersive X-ray spectroscopy (EDX) attached to the TEM was employed to probe the local atomic percentages of the samples. The sample was then patterned with an indium-tin oxide (ITO) electrode to construct a device with ITO/Ni-NiO/Si sandwich structure, and the device's photoresponses and *I–V* characterizations were probed by a Keithley 2400 source meter. The sample area is 9 mm^2. For *I–V*, the devices were measured under a forward bias mode. The photoresponse measurements were performed under UV illumination with a power of ∼21 mW/cm^2 (λ = 365 nm) in air at room temperature. The setup of the photoresponse measurements is illustrated in Fig. 1. The photocurrent was recorded each second by the Keithley 2400. To confirm that the probed photoresponses and *I–V* resulted solely from the Ni-NiO core-shell structure, a reference sample of ITO/Ni/Si was prepared. This was to rule out possible junction effects contributed by Ni/Si. In addition, in order to acquire the developing mechanism of the NiO layer, three samples with annealing conditions of 250°C for 15 minutes, 250°C for 30 minutes, and 250°C for 4 hr were prepared and probed by HRTEM.

Results and Discussion

The structural configurations of the Ni and Ni-NiO nano-arrays are presented in Figs. 2a and 2b, respectively. Both samples comprised freestanding and highly aligned nano-arrays, each being ∼70 nm in diameter and ∼350 nm in length. Two samples are found to display good connections with the Si substrate and exhibit columnar microstructure. This microstructure resulted from the Ni columns with commenced growth along the AAO walls and merged at the center of the pores, as described in our previous work.[27] We observed that manufacturing nano-array/wire structures using electro-deposition tends to produce segment structures with orientations parallel to the array/wire's long axis.[31,32] This is because the deposition is triggered at the electrode side and followed by growth along the long axis, due to the space

[z] E-mail: chih@cc.nctu.edu.tw

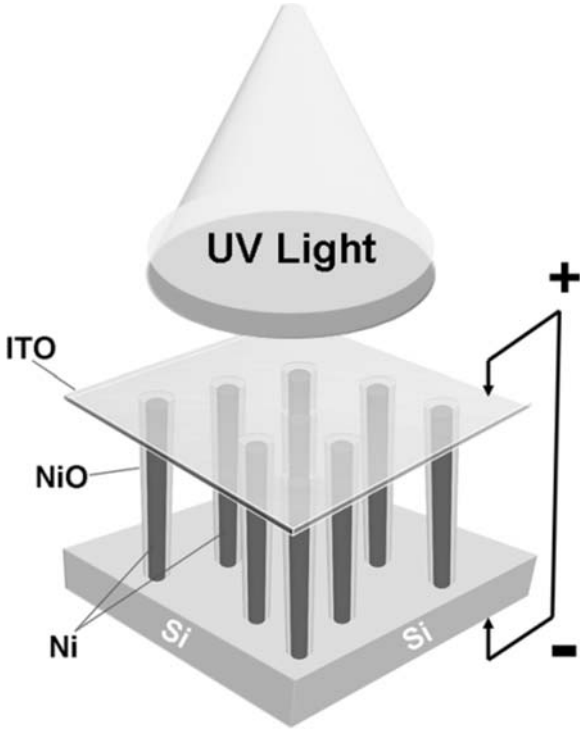

Figure 1. Setup of photoresponse characterization.

confinement of the array/wire. However, electroless deposition is an auto-catalytic process involving several simultaneous reactions in an aqueous condition. It may stimulate material growth wherever nucleation energy is low. The TEM results shown here and Fig. 2b of Liu et al.[27] reveal that the AAO wall provides a heterogeneous nucleation site for the deposition of Ni, which is therefore responsible for the columnar structure obtained in Fig. 2. The Ni-NiO sample, due to its heat-treatment, exhibits more homogeneity in microstructure than does the Ni sample. A thin layer covering the Ni arrays is marked in Fig. 2b, which is attributed to NiO as further confirmed by Fig. 3b.

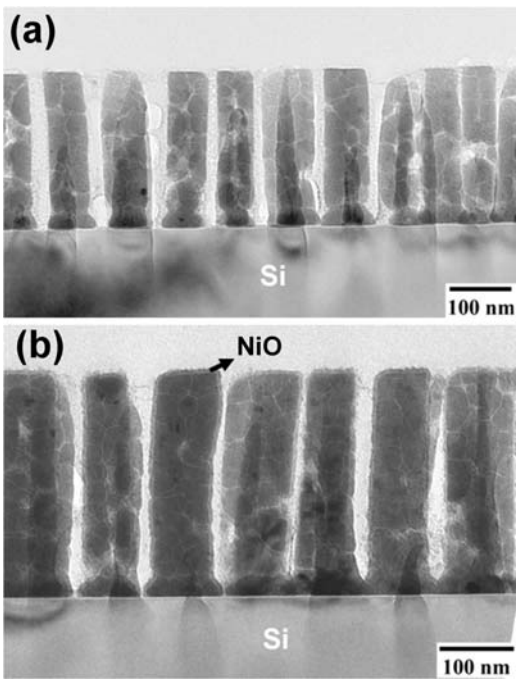

Figure 2. Cross-sectional TEM images of (a) Ni and (b) Ni-NiO nano-arrays on Si-substrates. Arrow of (b) indicates the NiO layer present at the Ni array surface.

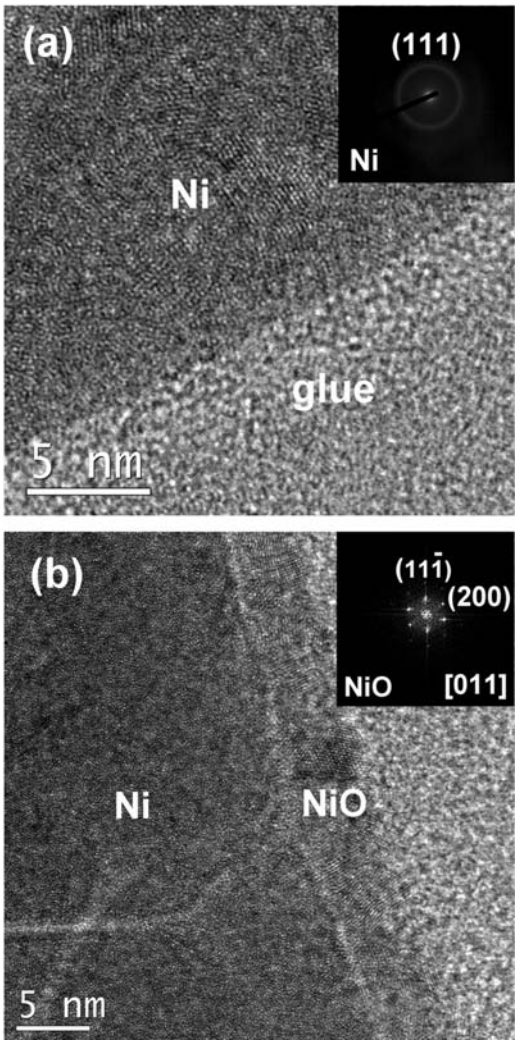

Figure 3. HRTEM images of (a) Ni and (b) Ni-NiO array surfaces. The insets of (a) and (b) demonstrate the SAD and FFT of the Ni and the NiO layer, respectively.

The microstructural details of the Ni and Ni-NiO sample surfaces are highlighted in Figs. 3a and 3b, respectively. The Ni array contains a nano-crystalline phase, as described in Ref. 27. The nano-crystalline phase is supported by the selected area diffraction (SAD) pattern, as depicted in the inset of Fig. 3a. Figure 3b shows that an NiO layer with a thickness of ∼5 nm is developed on the Ni array's surface upon annealing. NiO layers of similar thickness were seen elsewhere in the same sample, suggesting that the Ni-NiO core-shell structure is homogeneous in the sample. The crystallographic phase of NiO was verified by the fast Fourier transformation (FFT) mode, as demonstrated in the inset of Fig. 3b. The result is consistent with that acquired by the EDX, which shows Ni and O with approximate atomic percentages of 53% and 47%, respectively.

It is likely that the NiO layer is developed through an outward-diffusion mechanism, where the outward-diffusion rate of Ni is more efficient than the inward-diffusion rate of O upon annealing. The details of this mechanism have been described in the literature.[33,34] To better understand the development mechanism of NiO, the time-dependent microstructural evolution of the Ni/NiO interface was probed. The resulting microstructures of Ni array surfaces are summarized in Figs. 4a–4c, which reflect annealing at 250°C for 15 minutes,

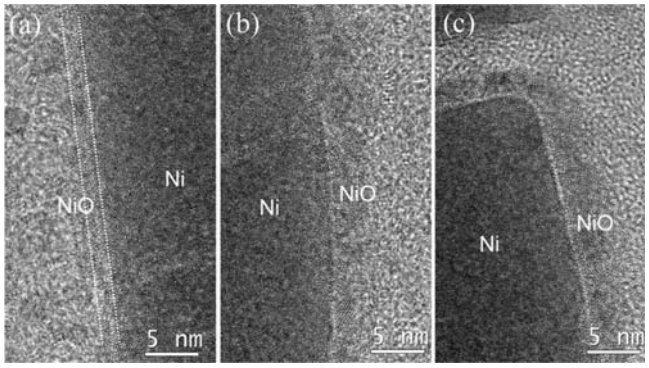

Figure 4. HRTEM images of Ni/NiO junction for annealing conditions of (a) 250°C 15 minutes (b) 250°C 50 minutes, and (c) 250°C 4 hr.

30 minutes, and 4 hr, respectively. Here, increasing the annealing time by 3.75 hr added only a layer of 1–2 nm thick to the NiO. However, comparing Fig. 3b with Fig. 4b shows that an increase of 50°C in annealing temperature can thicken the NiO layer by ∼3 nm, indicating that the formation of NiO is more dependent on annealing temperature than on annealing time. The NiO layer locates between the two dotted lines in Figure 4a. A boundary gradually formed between Ni and NiO and finally separated the core and shell physically. The boundary is likely to be the supersaturated phosphor resulting from the heat-treatment.[27,29,35] The emergence of the second phase boundary seems to be a barrier hindering further diffusion of Ni toward the surface with increase in annealing time, thus limiting the thickening of the NiO layer.

The I–V characteristics of ITO/Ni/Si and ITO/Ni-NiO/Si devices are highlighted in Fig. 5a. For ITO/Ni-NiO/Si, the exponential increase in current under forward bias indicates a Schottky contact, while the linear I–V of ITO/Ni/Si suggests an ohmic contact. The photocurrent increased abruptly to approximately 7 μA when the UV light was switched on. The photocurrent was about two orders in magnitude less than that produced at 2 V. However, it is very sensitive in detecting the UV light. By comparing these two I–V profiles, one can assign the Schottky characteristic to the nanojunction developed between Ni and NiO. The same conclusion was made by Zhao et al.,[36] who demonstrated a similar scenario with an NiO layer of ∼3 nm. Interestingly, both they and we independently found that a semiconducting NiO layer of 3–5 nm thick can develop a semiconductor-metal Schottky junction. Our results also show that the device does not show breakdown when 20 volts are applied. The thickness of the semiconducting layer in Zhao et al.[36] and in our study is much smaller than that generally seen in traditional semiconductor-metal-based devices.[37–39] Such discrepancy may be due to the junction of those traditional devices being developed by methods such as physical or chemical vapor deposition, which differ from that described in this work. Those traditional deposition technologies usually require several mono layers to form the bonding with the substrate in the very beginning of the deposition process. Only when the interfacial bonds are stabilized can further deposition be feasible. The deposition mechanism is illustrated in Fig. 5b, which is described as "top down" henceforth. It stacks one material onto another artificially, which inevitably results in a thick layer of the deposited material. Although semiconducting layers with order of thickness similar to ours have been reported, highly sophisticated facilities are usually required.[40,41]

However, we found that annealing causes the semiconducting NiO layer to be naturally formed at the expense of Ni. The mechanism can be called "bottom-up," as illustrated in Fig. 5c. This mechanism involves atomic diffusion where Ni moves toward the surface and is oxidized, leading to the emergence of an NiO layer at the array's surface. This mechanism is expected to produce a more robust connection across the junction than does the "top-down" mechanism, because the former internally induces one material (NiO) from within another

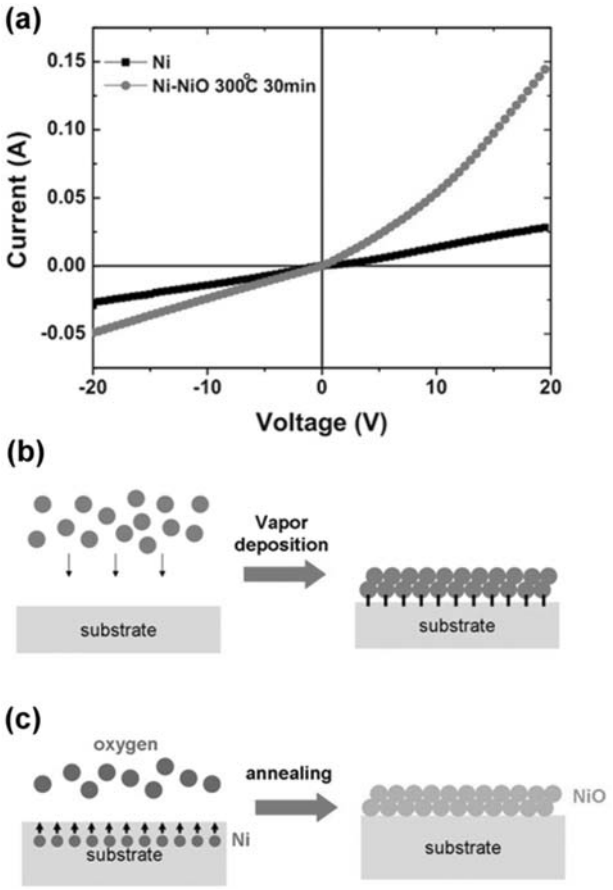

Figure 5. (a) *I–V* characteristics of ITO/Ni/Si and ITO/Ni-NiO/Si devices. (b) "Top-down" mechanism adopted in physical/chemical vapor depositions. (c)"Bottom-up" mechanism described in the development of NiO.

(Ni), instead of externally stacking two dissimilar materials. This explains why a Schottky nanojunction with an extra-thin NiO layer can be developed at the array surface. The quality of the junction is critical to a device's performance, because imperfections are likely to occur where two dissimilar materials are adjacent. Improving the quality of a junction remains a long-standing objective, and it is difficult to balance the quality and the scale of the junction. Our work hereby provides an option for achieving this goal. Nevertheless, we acknowledge that the presence of the second phase boundary may influence the quality of the Ni/NiO junction. Determining how to remove the boundary may depend on the conditions of the plating solutions and requires further investigation.

The photoresponses of two devices are highlighted in Fig. 6a. ITO/Ni-NiO/Si exhibits detectable photocurrent without an external bias. ITO/Ni/Si produced a zero response; hence, the photocurrent can be completely attributed to the presence of the Ni-NiO nanojunction. The sharp rising and falling of the signal in response to the UV light being on and off, respectively, show great potential for the device as a UV detector. The clear photoresponse is generated without the need of applied bias, thus saving energy. It is noteworthy that no external bias was used when UV light detection was measured in the current study. In previous studies related to UV light detection, an external bias had to be applied to the sensor material.[42,43] The reason for applying a voltage bias is that electron-hole pairs need to be separated after the UV light shines on the sensor material. If there is no external bias as the driving force, the electrons and holes would recombine, and no photocurrent would occur. The nanojunction in the Ni-NiO core-shells in the present study has a built-in voltage that can directly provide the driving force required for the movement of electrons and holes generated

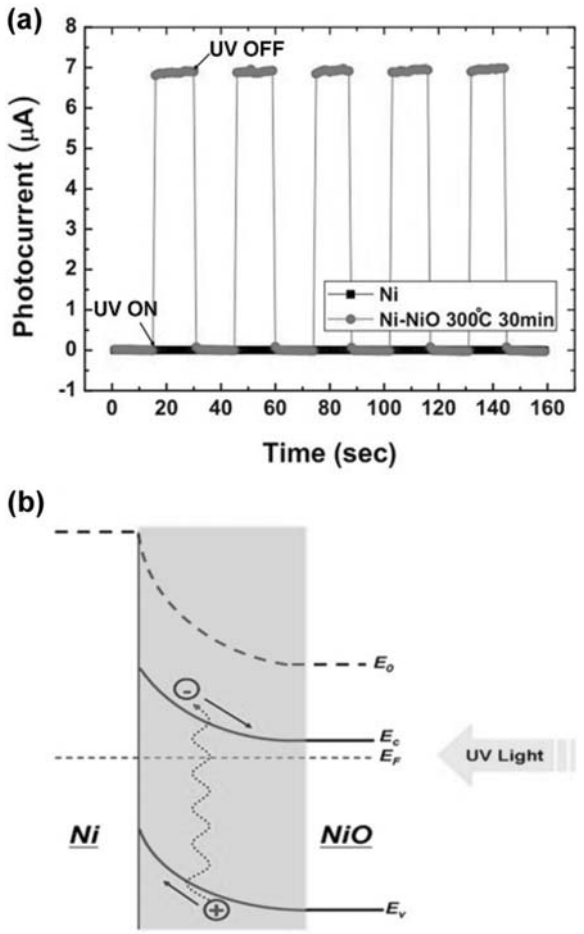

Figure 6. (a) The measured photoresponses for ITO/Ni/Si and ITO/Ni-NiO/Si devices. (b) Energy band diagram for the Ni-NiO nanojunction, with an UV-light illumination taking place at the NiO side. The colorful box highlights the depletion region where the photo-carriers are generated and regulated.

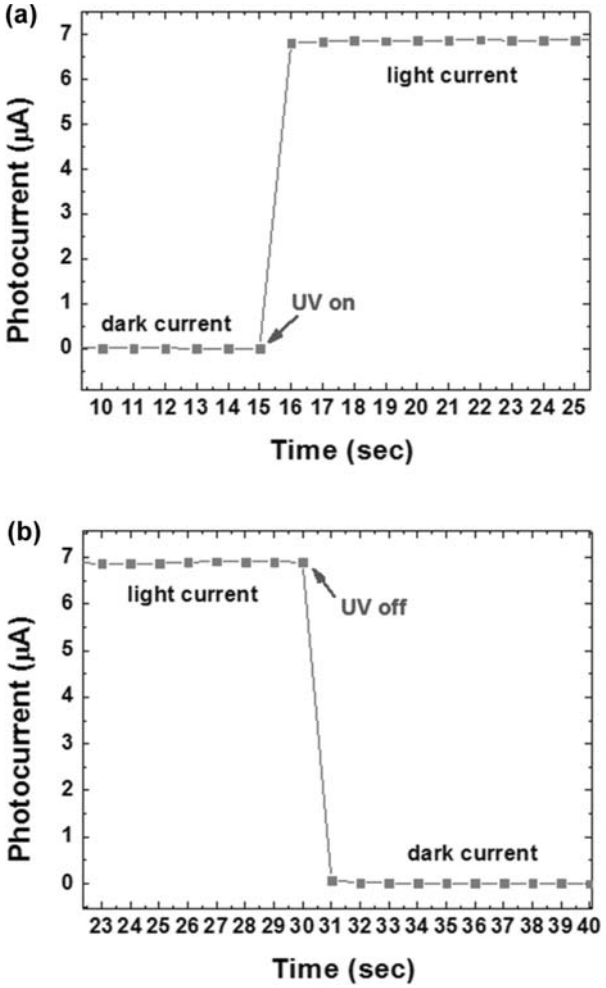

Figure 7. Selected features of the photocurrent's response to (a) light-on and (b) light-off.

by the UV light. The energy band diagram is shown schematically in Fig. 6b. There is a depletion region at the interface between Ni and NiO. From the diagram, it is proposed that when the UV light shines on the NiO shells, electron-hole pairs can be generated in NiO. Since the built-in voltage at the Ni-NiO junction pushes the electrons to move toward the NiO and holes to migrate toward the Ni core, a photocurrent takes place. It is noteworthy that ITO was used as the upper electrode and hetero-junctions of ITO-NiO would form. Thus, these hetero-junctions may also affect the photocurrent. However, the junction area of Ni-NiO is 16 times larger than that of ITO-NiO. The calculation was performed using the following equation:

$$\frac{Ni - NiO\ junction\ area = (2\pi \times r_{Ni} \times h_{Ni}) + \left(\pi \times r_{Ni}^2\right)}{ITO - NiO\ junction\ area = \pi \times (r_{Ni} \times t_{NiO})^2} \quad [1]$$

where r is radius of the Ni nanorod, h is height of the Ni nanorod and t is thickness of the NiO shell. Therefore, we could neglect the influence from ITO-NiO junctions. In addition, it is reported that the Ni core has a high reflection rate of 41.2% on UV light.[44] Therefore, when the UV light shines on the NiO-Ni core shells, some of the UV light is absorbed by the NiO shells. The transmitted UV light hits the Ni cores and some of the light is reflected. Some of the reflected UV light can be absorbed again by the NiO shells. Therefore, the light absorption efficiency may be higher for the Ni-NiO core-shells.

Figures 7a and 7b depict selected features of Fig. 6a and further examine the photocurrent's response to light-on and light-off, respectively. The device clearly responds to the UV-light illumination in less than one second. This rapid photoresponse is ascribed to the highly depleting region of the Ni/NiO Schottky nanojunction, where the carriers are pumped through the junction immediately and the charge recombination probability is reduced. This conjecture is supported by Chen et al.,[45] who independently demonstrated a similar conclusion for TiO_2-Pt Schottky contact. The device's instant response to the UV light is superior to the time-delay photoresponses obtained in several well-known photoconductive compounds.[16,17,46–49] In addition, a steady photocurrent with UV light-on is obtained, which is advantageous to the design of the UV detector. The steady photocurrent is likely to be associated with the one-dimensional configuration of the array, because it provides a confined transportation path for the photocarriers.[50]

Conclusions

The work provides a simple method for fabricating nanostructured UV photodetectors, in the hope of reducing manufacturing cost while being environmental friendly. We have demonstrated the electrical and photoconductive properties of Ni-NiO core-shell nano-arrays. The correlations between the array's properties and microstructure were also explored. NiO is developed from the oxidation of Ni that takes place at the array's surface. Annealing temperature was found to determine the formation of NiO. The formed Ni/NiO interface naturally establishes a Schottky nanojunction, which is responsible for the detected electrical and photoconductive properties. Capped with an ITO electrode, the core-shell structure takes advantage of its

large junction area and yields photocurrent under UV illumination without an external bias. The photoresponse of the device is fast and steady, showing great potential for use as a UV detector.

Acknowledgment

The authors thank Frontier Photonics Research Center/UST at National Chiao Tung University for financial support.

References

1. K. Makise, K. Mitsuishi, M. Shimojo, and K. Furuya, *Nanotechnology*, **20**, 425305 (2009).
2. S. A. Mcdonald, G. Konstantatos, S. Zhang, P. W. Cry, J. D. Klem, L. Levina, and E. H. Sargent, *Nature Mater.*, **4**, 138 (2005).
3. M. Razeghi and A. Rogalski, *J. Appl. Phys.*, **79**, 7433 (1996).
4. J. D. Prades, R. Jimenez-Diaz, F. Hernandez-Ramirez, S. Barth, A. Cirera, A. Romano-Rodriguez, S. Mathur, and J. R. Morante, *Sensors and Actuators B, Chemical*, **140**, 337 (2009).
5. Y. L. Chueh, C. H. Hsieh, M. T. Chang, L. J. Chou, C. S. Lao, J. H. Song, J. Y. Gau, and Z. L. Wang, *Adv. Mater.*, **19**, 143 (2007).
6. S. M. Peng, Y. K. Su, L. W. Ji, C. Z. Wu, W. B. Cheng, and W. C. Chao, *J. Phys. Chem. C.*, **114**, 3204 (2010).
7. K. M. Noone and D. S. Glnger, *ACS Nano.*, **3**, 261 (2009).
8. I. Mhaidat, S. Hamilakis, C. Kollia, A. Tsolomitis, and Z. Loizos, *Mater. Lett.*, **62**, 4198 (2008).
9. G. Konstantatos, I. Howard, A. Fischer, S. Hoogland, J. Clifford, E. Klem, L. Levina, and E. H. Sargent, *Nature.*, **442**, 180 (2006).
10. Y. Li, F. D. Valle, M. Simonnet, I. Yamada, and J. J. Delaunay, *Nanotechnology*, **20**, 45501 (2009).
11. Z. Hu, Q. Chen, Z. Li, Y. Yu, and L. M. Peng, *J. Phys. Chem. C.*, **114**, 881 (2010).
12. T. Zhai, L. Li, X. Wang, X. Fang, Y. Bando, and D. Golberg, *Adv. Funct. Mater.*, **20**, 4233 (2010).
13. C. Soci, A. Zhang, B. Xiang, S. A. Dayeh, D. P. R. Aphin, J. Park, X. Y. Bao, Y. H. Lo, and D. Wang, *Nano Lett.*, **7**, 1003 (2007).
14. M. Xia, Q. Zhang, H. Li, G. Dai, H. Yu, T. Wang, B. Zhou, and Y. Wang, *Nanotechnology*, **20**, 55605 (2009).
15. J. S. Jie, W. J. Zhang, Y. Jiang, X. M. Meng, Y. Q. Li, and S. T. Lee, *Nano Lett.*, **6**, 1887 (2006).
16. S. Mridha, M. Nandi, A. Bhaumik, and D. Basak, *Nanotechnology*, **19**, 275705 (2008).
17. W. S. Wang, T. T. Wu, T. H. Chou, and Y. Y. Chen, *Nanotechnology*, **20**, 135503 (2009).
18. K. Black, A. C. Jones, I. Alexandrou, P. N. Heys, and P. R. Chalker, *Nanotechnology*, **21**, 45701 (2010).
19. W. Yan, N. Mechau, H. Hahn, and R. Krupke, *Nanotechnology*, **21**, 115501 (2010).
20. S. Dalui, C. C. Lin, H. Y. Lee, S. F. Yen, Y. J. Lee, and C. T. Lee, *J. Electrochem. Soc.*, **157**, H516 (2010).
21. S. Y. Chang, N. H. Yang, and Y. C. Huang, *J. Electrochem. Soc.*, **156**, K200 (2009).
22. R. Ghosh, M. Dutta, and D. Basak, *Appl. Phys. Lett.*, **91**, 73108 (2007).
23. X. Cao, H. Zeng, M. Wang, X. Xu, M. Feng, R. Ghosh, M. Dutta, and D. Basak, *J. Phys. Chem. C*, **112**, 5267 (2008).
24. G. Konstantatos, L. Levina, J. Tang, and E. H. Sargent, *Nano Lett.*, **8**, 4002 (2008).
25. S. N. Das, K. J. Moon, J. P. Kar, J. H. Choi, J. Xiong, T. Lee, and J. M. Myoung, *Appl. Phys. Lett.*, **97**, 22103 (2010).
26. T. Y. Wei, C. T. Huang, B. J. Hansen, Y. F. Lin, L. J. Chen, S. Y. Liu, and Z. L. Wang, *Appl. Phys. Lett.*, **96**, 13508 (2010).
27. C. M. Liu, Y. C. Tseng, C. Chen, M. C. Hsu, T. Y. Chao, and Y. T. Cheng, *Nanotechnology*, **20**, 415703 (2009).
28. C. M. Liu, C. Chen, and H. E. Cheng, *J. Electrochem. Soc.*, **158**, K58 (2011).
29. T. K. Tsai and C. G. Chao, *Appl. Surf. Sci.*, **233**, 180 (2004).
30. S. Han, H. Y. Chen, C. C. Chen, T. N. Yuan, and H. C. Shin, *Mater. Lett.*, **61**, 1105 (2007).
31. F. Tian, J. Zhu, and D. Wei, *J. Phys. Chem. C*, **111**, 12669 (2007).
32. S. Han, H. Y. Chen, C. C. Chen, T. N. Yuan, and H. C. Shin, *Mater. Lett.*, **61**, 1105 (2007).
33. P. Kofstad, *High-Temperature Oxidation of Metals*, John Wiley & Sons, New York 1966.
34. R. Nakamura, J. G. Lee, H. Mori, and H. Nakajima, *Phil. Mag.*, **88**, 257 (2008).
35. C. M. Liu, W. L. Liu, S. H. Hsieh, T. K. Tsai, and W. J. Chen, *Appl. Surf. Sci.*, **243**, 259 (2005).
36. X. Zhao, J. L. Sun, and J. L. Zhu, *Appl. Phys. Lett.*, **93**, 152107 (2008).
37. A. J. Mathai and D. Patel, *Crys. Res. Technol.*, **45**, 717 (2010).
38. V. W. L. Chin, J. W. V. Storey, and M. A. Green, *Solid-State Electronic*, **39**, 277 (1996).
39. F. Via, P. Lanza, O. Viscuso, G. Ferla, and E. Rimini, *Thin Solid Films*, **161**, 13 (1988).
40. W. Y. Park, G. H. Kim, J. Y. Seok, K. M. Kim, S. J. Song, M. H. Lee, and C. S. Hwang, *Nanotechnology*, **21**, 195201 (2010).
41. N. Sirikulrat, *Appl. Phys. Lett.*, **92**, 62115 (2008).
42. W. Yan, N. Mechau, H. Hahn, and R. Krupke, *Nanotechnology*, **21**, 115501 (2010).
43. K. T. Lee, A. S. C. Maria, and G. Han, *J. Phys. Chem. C*, **112**, 69 (2008).
44. ASM, *Metals Handbook*, eighth ed, 1976.
45. H. Chen, S. Chen, X. Quan, H. Yu, H. Zhao, and Y. Zhang, *J. Phys. Chem. C*, **112**, 9285 (2008).
46. Y. Han, G. Wu, M. Wang, and H. Chen, *Polymer*, **51**, 3736 (2010).
47. J. P. Kar, S. N. Das, J. H. Choi, Y. A. Lee, and J. M. Myoung, *J. Crys. Grow.*, **311**, 3305 (2009).
48. K. Tsuji, K. Hayashi, J. H. Kaneko, F. Fujita, A. Homma, Y. Oshiki, T. Sawamura, and M. Furusaka, *Diamond Relat. Mater.*, **14**, 2035 (2005).
49. M. Yang, J. L. Zhu, W. Liu, and J. L. Sun, *Nano Res.*, in press.
50. J. Zou, Q. Zhang, K. Huang, and N. Marzari, *J. Phys. Chem. C*, **114**, 10725 (2010).